European Review for Medical and Pharmacological Sciences 2021; 25: 7285-7296

Thymosin β4 and β10 are highly expressed at the deep infiltrative margins of colorectal cancer – A mass spectrometry analysis

A. OLIANAS[1], S. SERRAO[1], V. PIRAS[1], B. MANCONI[1], C. CONTINI[1], F. IAVARONE[2,3], G. PICHIRI[4], P. CONI[4], L. ZORCOLO[5], G. ORRÙ[5], I. MESSANA[6], G. FAA[4,7], M. CASTAGNOLA[8], D. FANNI[4], T. CABRAS[1]

[1]Department of Life and Environmental Sciences, University of Cagliari, Cagliari, Italy
[2]Department of Basic, Intensive and Perioperative Clinic Biotechnological Sciences, Catholic University of Sacred Heart, Rome, Italy
[3]Foundation of University Hospital "A. Gemelli", IRCCS, Rome, Italy
[4]Department of Medical Sciences and Public Health, Division Pathological Anatomy, Cagliari, Italy
[5]Department of Surgical Sciences, University of Cagliari, Cagliari, Italy
[6]Institute of Chemical Sciences and Technologies "Giulio Natta", National Council of Research, Rome, Italy
[7]Adjunct Professor Department of Biology, College of Science and Technology, Temple University, Philadelphia, PA, USA
[8]Laboratory of Proteomics, European Center of Brain Research, IRCCS Fondazione Santa Lucia, Rome, Italy

A. Olianas and S. Serrao contributed equally to this work and share first authorship

D. Fanni and T. Cabras contributed equally to this work and share last authorship

Abstract. – OBJECTIVE: Colorectal cancer (CRC) is a complicated tumor, involving several oncogenic signaling pathways, and with a molecular mechanism not fully understood yet. The implication of thymosin β4 (Tβ4) with tumor insurgence and in migration of CRC cells was evidenced in the past with different methodologies, while Tβ10 connection with CRC has been sporadically investigated. This study focused on the implication of both types of thymosin in CRC progression and invasion by analyzing the changes in their levels according to different zones of the tumor, and to Dukes stage and budding index.

PATIENTS AND METHODS: Tβ4 and Tβ10 were analyzed in deep and superficial tumor samples, and normal mucosa from 18 patients. Concentrations of Tβ4 and Tβ10 have been measured by high-pressure liquid chromatography (HPLC) coupled to electrospray-ion trap mass spectrometry (ESI-IT-MS). MS data were compared by *t*-test and ANOVA statistical analysis. Identification of thymosin and their proteoforms has been performed by HPLC-high resolution-ESI-IT-MSMS.

RESULTS: Both Tβ4 and Tβ10, exhibited intra-tumoral quantitative differences, being upregulated in the deep part of the CRC. They exhibited, moreover, strong association with the Dukes stage and the budding grade, being more concentrated in patients at Dukes stage B and with budding index "2".

CONCLUSIONS: The results obtained in the present investigation encouraged the hypothesis that the two thymosin are involved in colorectal cancer progression, and in promoting cancer invasion. Thus, they are good candidates to be diagnostic/prognostic biomarkers and therapy targets.

Key Words:
Colorectal cancer, Intra-tumor heterogeneity, Mass spectrometry, Thymosin β4, Thymosin β10.

Introduction

Thymosin are a family of peptides/proteins with dimensions ranged between 1kDa and 15 kDa, isolated for the first time from the calf thymus[1]. Among them, thymosin beta4 (Tβ4) and beta10 (Tβ10) are ubiquitously expressed by several cells and organs[2,3]. Tβ4 and Tβ10 play a crucial role in human physiopathology. In particular, they considered moonlighting peptides involved in many physiological processes, such

Corresponding Author: Daniela Fanni, MD, Ph.D; e-mail: daniela.fanni@unica.it

as the cellular proliferation and differentiation, cellular healing and regeneration, apoptosis, angiogenesis, embryogenesis and organ growth[2,4,5]. Tβ4 and Tβ10 activities are mainly linked to their ability to modulate the cytoskeleton organization through the interaction with G-actin monomers, and the regulation of assembling-disassembling of actin filaments[2,5,6]. Tβ4 role was investigated in carcinogenesis and tumor progression[7,8], in particular, Tβ4 and Tβ10 expression has been studied in different solid tumors, including gastrointestinal stromal tumor[9], hepatocellular carcinoma[10], and colorectal cancer (CRC)[11-14]. Despite the advances in the knowledge and understanding of its insurgence and progression, CRC remains globally one of the most common and malignant neoplasia[15,16]. It is known that CRC is a multifaceted tumor, involving several oncogenic signaling pathways, but the comprehensive understanding of the molecular mechanisms associated are still a challenge.

It was demonstrated that Tβ4 can facilitate metastasis and tumor angiogenesis[17] by regulating cancer cell hypoxia[18-19] through the expression of vascular endothelial growth factor, and hypoxia inducible factor-1α[20]. Moreover, the ability of Tβ4 to promote the survival of cells seems to favor tumoral growth. This ability is due to the protection from oxidative stress[21], caspase inhibition[22], and anti-apoptotic action[23]. For this reason, Tβ4 has been candidate as molecular target for anti-tumor therapy[24,25].

The ability of Tβ4 to stimulate the process of epithelial-mesenchymal transition (EMT), and, thus, cellular migration[12,26], may be essential for both embryogenesis and the acquisition of metastatic capacity of neoplastic cells[8]. Tβ4-triggered EMT is considered the main event inducing the invasion and migration of CRC cells[12,27-30]. In addition, the overexpression of Tβ4 was associated to the insurgence of distant metastases in carriers of CRC[31].

The biological role of Tβ10 has been less investigated than that of Tβ4. However, despite marked structural and functional similarities, it has been proposed that the two peptides show completely different biological functions[32]. As already reported, Tβ4 promotes angiogenesis[5,17], whereas Tβ10 has been shown to inhibit angiogenesis by interfering with Ras function[33]. While Tβ4 facilitates cell migration, Tβ10 has been shown to inhibit cell migration of human endothelial cells[34]. Furthermore, Tβ4 plays a relevant anti-apoptotic role by preventing apoptotic cell death[24,25] although Tβ10 has been shown to accelerate apoptosis[35]. Tβ10 activity appears different in diverse tumors, and in some cases, opposite to Tβ4. Studies on different types of tumors have reported controversial and sometimes opposite effects of Tβ10. In ovarian cancer, the overexpression of Tβ10 was associated to inhibition of angiogenesis and tumor growth[33], and to high levels of apoptosis inducing the slowdown of tumor cell growth[36]. Overexpression of Tβ10 was associated to the suppression of cell migration and metastasis in cholangiocarcinoma[37]. On the contrary, Tβ10 overexpression was related with proliferation, invasion, and distant metastasis in breast cancer cells *in vitro* and *in vivo*[38,39], as well as in pancreatic cancer[40], non-small cell lung cancer[41], and hepatocellular carcinoma[10]. Another study[42] highlighted high expression of Tβ10 in colon cancer cells.

Considering the properties of Tβ10 and Tβ4, and their activities in malignant progression of tumors, we believed interesting to deepen the study on their implication in CRC invasion and progression. For this purpose, we investigated both Tβ10 and Tβ4, and some of its proteoforms, by high-performance liquid chromatography (HPLC) coupled to mass spectrometry (MS), in relation to the different tumor zones (superficial and deep tumor), and to the Dukes staging. As internal control, we utilized the surrounding normal colon mucosa collected from the same patients analyzed in this study.

Patients and Methods

Reagents and Apparatus

All chemicals and reagents used were from analytical grade and were purchased from Sigma Aldrich (St. Louis, MI), Merck (Darmstadt, Germany). Tβ4 standard peptide was purchased from Bachem (Bubendorf, Swiss). HPLC-Low Resolution (LR)-ESI-MS measurements were carried out by a Surveyor HPLC system (ThermoFisher, San Jose, CA, USA) connected to a LCQ Advantage mass spectrometer (ThermoFisher Scientific San Jose, CA, USA). The chromatographic column was a reversed-phase (RP) Vydac 208MS-C8 (Hesperia, CA, USA) with 5 μm particle diameter (150x2.1 mm). HPLC-High Resolution (HR)-ESI-MS/MS experiments were carried out using an Ultimate 3000 Micro HPLC apparatus (Dionex, Sunnyvale, CA, USA) equipped with a FLM-3000-Flow manager module and coupled to

an LTQ Orbitrap XL apparatus (ThermoFisher Scientific San Jose, CA, USA). The column was a Zorbax 300SB-C8 column (3.5 μm particle diameter; 1.0 × 150 mm) for the top-down analysis.

Study Subjects

The study included 18 patients submitted to surgical resection of colorectal tumors by the unit of Colorectal Surgery of the Department of Surgical Sciences (Cagliari University, Italy). Ethics Committee approval was obtained for the study (Protocol No. 2020/10912 – code: EMIB-IOCCOR) and full written consent forms were obtained from the donors.

Colon cancer was included when characterized by budding margins with evident morphological signs of epithelial-mesenchymal transition. Clinical and demographic data of the 18 patients are reported in Table I. 8 females and 10 males were included in the study with average age ± standard deviation (SD) 66 ± 12, and 72 ± 9, respectively. The vast majority of tumors were characterized by infiltrative margins, with the exception of three, which showed expansive margins. Patients were classified as A, B or C according with the Dukes stage: four patients were in stage A (carcinoma limited to the wall of the rectum), eight patients were designed as B stage (cancer in direct continuity to the extra-rectal tissue), and six patients as C stage (metastases present in the regional lymph nodes). As it concerns the tumor budding index, namely the presence of de-differentiated single cells or small clusters of up to five cells at the invasive front of CRC[43], it was absent (0) in three patients, slight (1) in six patients, discreet (2) in three patients and marked (3) in six patients.

Preparation of Samples for HPLC-ESI-MS Analysis

Three kinds of tissues were collected from each patient: i) the surface layer of the tumor, named "S" in the results; ii) the deep layer of the tumor, "D"; iii) the healthy colon mucosa, "H". The three different tissue samples were of different sizes (but not exceeding 1 × 1 cm). The protein extraction was performed on fresh tissues, indeed, immediately after the surgical resection. Tissue samples were washed from blood residues with a physiological solution and dipped in 600 μL of extraction buffer to be homogenized in an ice bath. The extraction buffer was composed as follows: 25 mM Hepes pH 7.8, 50 mM KCl, beta-Octyl-glucopyranoside 0.2%, 1 mM dithiothreitol. To inhibit proteases one Mini-Complete™ tablet (Roche Diagnostics, Basel, Swisse) was added to 10 mL of buffer. The homogenization was performed with Ultra Turrax apparatus and followed by three cycles of 5 min in a sonication bath. The homogenized tissues were centrifuged at 19000 g, 4°C for 10 min and the supernatant used to the following fractionation step. An aliquot of 5 μl of the supernatant was used for determining the total protein concentration by Bicinchoninic Acid (BCA) assay (QuantiPro BCA micro-assay kit, from Sigma-Aldrich, Mer-

Table I. Demographic and clinical information, type of tumor, Dukes stage, and budding index of each patient included in the study.

Patients	Gender and age	Type of tumor	Dukes Stage	Budding
#1	F, 59 yr	Infiltrating	C	3
#2	F, 79 yr	Infiltrating	B	3
#3	M, 78 yr	Infiltrating	B	3
#4	F, 55 yr	Infiltrating	B	2
#5	M, 83 yr	Infiltrating	B	1
#6	M, 70 yr	Infiltrating	B	2
#7	F, 81 yr	Infiltrating	A	0
#8	M, 75 yr	Infiltrating	B	1
#9	M, 66 yr	Infiltrating	B	3
#10	F, 52 yr	Infiltrating	C	1
#11	M, 52 yr	Infiltrating	C	3
#12	M, 64 yr	Infiltrating	C	3
#13	M, 76 yr	Expansive	A	1
#14	F, 59 yr	Infiltrating	C	0
#15	M, 76 yr	Infiltrating	C	1
#16	M, 80 yr	Infiltrating	A	0
#17	F, 66 yr	Expansive	B	2
#18	F, 80 yr	Expansive	A	1

ck KGaA, Darmstadt, Germany). The resulting concentrations were corrected based on initial volumes of the raw extracts recovered after homogenization and expressed as mg/mL.

The samples were, then, submitted to three cycles of ultrafiltration with 30 kDa cut-off membranes (Amicon® Ultra Centrifugal Filters, Merck-Millipore, MA, USA), for the second and third cycle the >30 kDa fraction, retained by the membrane, was solubilized in 200 µL of a hydro-organic (HO) solution (0.05% trifluoroacetic acid (TFA), and 20% acetonitrile (ACN)) before repeating the ultrafiltration. <30 kDa fractions obtained from each ultrafiltration cycle were unified in a single volume and, to eliminate the components of the extraction buffer, it was dialyzed in 25 mM sodium acetate buffer pH 4.3, under stirring at 4°C for 3 hours, using dialysis devices with a molecular cut-off of 500 Da (Float-A-Lyzer G2, Sigma-Aldrich, Merck KGaA, Darmstadt, Germany). After dialysis, the samples were lyophilized, and the powder suspended in 100 µL of 0.1% aqueous TFA. At the end of the ultrafiltration cycles the >30kDa fraction recovered were solubilized in 100 µl of the HO-solution sonicated with 2 cycles of 5 min and then, centrifuged at 13000 rpm, 4°C for 10 minutes. The <30kDa and >30kDa fractions were immediately analyzed by HPLC-ESI-MS or stored at -80°C for the further analysis.

RP-HPLC-Low Resolution-ESI-MS Analysis

RP-HPLC-(LR)-ESI-MS analysis was performed on the 18 S, D, and H samples from the CRC patients (n = 18), by injecting 33 µL from each <30kDa and >30kDa fractions. The chromatographic separation was carried out using the eluents: A (0.056% TFA acidic solution), and B (acetonitrile/water 80:20 with 0.05% TFA). The gradient applied for the analysis was linear from 0 to 55% of B in 40 min, and from 55% to 100% of B in 10 min, at a flow rate of 0.1 mL/min entirely addressed to the ESI source. During the first 5 minutes of the analysis, the eluate was discharged to avoid that the high salt concentration could damage the instrument. Mass spectra were collected every 3 ms in the m/z range 300-2000 in positive ion mode. The MS spray voltage was 5.0 kV, and the capillary temperature was 260°C. MS resolution was 6000. With the same conditions, the Tβ4 standard peptide at different concentrations (0.005, 0.025, 0.05, 0.10, 0.25, 0.35, 0.5, 0.75, 1.00, 1.25, 1.50 µM) were injected in HPLC-(LR)-MS. Tβ4 and Tβ10 were searched along the total ion current (TIC) profile by using the extracted ion current (XIC) approach. The specific multiply-charged ions of the both peptides, and those of their derivatives from post-translational modifications (PTMs), are reported in Table II, with the experimental and theoretical average mass values (Mav) and the related retention times. Experimental mass values of all peptides were obtained using the MagTran 1.0 software[44]. The experimental values were compared with the theoretical masses of the peptides present at the human UniProtKB Data Bank (https://www.uniprot.org/). The experimental Mav value and the elution time of Tβ4 was compared also with those of the standard peptide. The selected multiply charged ions were chosen by excluding common values with other closely eluting proteins (± 0.5 m/z).

Quantitative Analysis

XIC peaks were considered for quantitative analysis when the signal-to-noise ratio was up to 5. XIC peak areas were integrated by using the following peak parameters: baseline window 15; area noise factor 50; peak noise factor 50; peak height 15% and tailing factor 1.5. The XIC peak area of a protein is proportional to its concentration[45,46], and, thus, useful in constant analytical conditions for the relative quantification of the same protein in different samples. The areas of XIC peaks have been corrected on the basis of the total protein concentrations measured in the total extracts. The areas of XIC peaks were correlated to the concentrations expressed in µM, on the base of the linear regression between the known concentrations of the standard Tβ4 and the respective XIC peak areas obtained by HPLC-(LR)-ESI-MS analysis (**Supporting information, Supplementary Figure 1**). The same slope was used to estimate the Tβ10 concentration, due to the high structural similarity of these two peptides.

To compare S, D and H samples statistical analyses have been performed with GraphPad Prism (5.0 version, La Jolla, CA, USA). The parametric *t*-test was applied, as well as the 1-way ANOVA with the Tukey's multiple comparison post-test. To analyze the samples in relation to the different Dukes stage and the budding index, the total tumor samples (S and D) of each patient were considered. Thus, we analyzed eight S and D tumor samples from the four patients at Dukes stage A, sixteen S and D samples for stage B, and twelve S and D samples for stage C. Analogous-

Table II. UniProtKB code, elution times (ET), monoisotopic (M) and Mav values (experimental and theoretical, Da), multiply-charged ions fragmented in high-resolution MS/MS experiments, of the Tβ4 and Tβ10 peptides and of their modified proteoforms, and multiply-charged ions used for XIC search and quantification by HPLC-low resolution-ESI-MS.

Peptide (UniProtKB code)	PTM	ET (min)	Experimental monoisotopic M (theoretical) (Da)	High-resolution MS/MS m/z (charge)	Experimental Mav (theoretical) (Da)	m/z ions selected for XIC
Tβ4 (P62328)	Nα-acetylated	19.3-19.8	4960.49 ± 0.08 (4960.48)	1241.13 (+4); 993.11 (+5); 827.76 (+6)	4962.8 ± 0.6 (4963.5)	1655.5, 1241.9, 993.7
	Fragm. 1-41	19.6-20.1	4744.43 ± 0.08 (4745.42)	792.08 (+6)	4746.7 ± 0.6 (4747.3)	1583.4, 1187.8, 950.5
	Met6-sulfoxide	17.4-18.0	4976.49 ± 0.08 (4976.48)	830.42 (+6)	4978.8 ± 0.6 (4979.5)	166.08, 1245.9, 996.9
	Lys16,25-Nε-diacetylated	21.2-21.6	5044.51 ± 0.08 (5044.51)	1010.51 (+5); 842.09 (+6)	5046.9 ± 0.6 (5047.6)	1683.3, 1262.7, 1010.5
Tβ10 (P63313)	Nα-acetylated	20.3-20.6	4933.54 ± 0.08 (4933.52)	823.26 (+6) 705.79 (+7)	4935.9 ± 0.6 (4936.5)	1646.3, 1235.1, 988.3
	Fragm. 1-41	20.0-20.7	4733.42 ± 0.08 (4733.41)	790.24 (+6)	0	1579.6, 1185.1, 948.3
	Met6-sulfoxide	20.3-20.9	4949.53 ± 0.08 (4949.52)	825.93 (+6)	4952.1 ± 0.6 (4952.5)	1651.8, 1239.1, 991.5

ly, the total tumor samples were considered to analyze the MS data in relation to budding index. We included six S and D tumor samples from three patients at budding index "0", twelve S and D samples from the budding "1" subgroup, six S and D samples from the budding "2" subgroup, and twelve S and D samples from the budding "3" subgroup. The nonparametric Mann-Whitney test has been applied. The nonparametric 1-way ANOVA was also applied with the Dunn' Multiple comparison post-test. Statistical analysis was considered to be significant when the *p*-value was <0.05.

Top-Down RP-HPLC-High Resolution-ESI-MS/MS Analysis

A volume of 20 µL of the <30kDa fraction from 3 samples were submitted to HPLC-(HR)-ESI-MS/MS analysis by using a top-down approach. Eluents were: A, 0.1% aqueous formic acid solution, and B, 0.1% aqueous formic acid solution in acetonitrile/water 80:20 v/v. The applied gradient was from 5 to 55% B in 40 min, from 55 to 100% B in 2 min, from 100 to 5% B in 2 min for a total acquisition time of 61 min at a flow rate of 80 µL/min. The MS spectra were acquired in data-dependent mode in the m/z range from 150 to 2000. The three most abundant ions were selected and fragmented by using collision-induced dissociation (CID, 35% normalized collision energy for 30 ms, with an isolation width of 6-10 m/z, activation q of 0.25). MS and MS/MS scans were acquired at a resolution of 60000. The capillary temperature was set to 250°C, source voltage 4 kV. Data were generated by Xcalibur 2.2 SP1.48 (ThermoFisher Scientific, Waltham, MA, USA) using default parameters of the Xtract program for the deconvolution. MS/MS data were analyzed by the Proteome Discoverer software (version 1.4.1.14, ThermoFisher Scientific, Waltham, MA, USA), based on SEQUEST HT cluster as search engine against UniProtKB human database (163,117 entries, release 2018_02). For peptide matching, high-confidence filter settings were applied: the peptide score threshold was 2.3; target FDR was: 0.01 (strict), 0.05 (relaxed). The limits for FDR setting were Xcorr scores greater than 1.2 for singly charged ions and 2.0 and 2.5 for doubly and triply charged ions, respectively. Precursor mass search tolerance was 10 ppm and fragment mass tolerance 0.8 Da. The following modifications were searched: phosphorylation, acetylation, oxidation of methionine residues. Peptide sequences

and sites of covalent modifications were also validated by manual inspection of the deconvoluted fragmentation spectra against the theoretical ones generated by MS-Product software, available at the ProteinProspector Web site (http://prospector.ucsf.edu/prospector/mshome.htm). The MS data have been deposited to the ProteomeXchange Consortium (http://www.ebi.ac.uk/pride) *via* the PRIDE[47,48] partner repository with the dataset identifier PXD027106.

Results

MS Top-Down Characterization

Two peaks eluting at 19.3-19.8 and 20.3-20.7 min and corresponding to peptides with Mav of 4962.8 ± 0.6, and 4935.9 ± 0.6 Da (Table II), were attributed to Tβ4 and Tβ10, respectively. Elution time and Mav of Tβ4 were in accordance with those obtained by HPLC-ESI-MS analysis of the standard peptide. Attributions were confirmed by high-resolution top-down MS/MS fragmentation of the multiply charged ions reported in Table II.

In addition to Tβ4 and Tβ10 peptides, several modified proteoforms were also characterized (Table II). The 1-41 fragment, and the Met6-sulfoxide derivatives of both Tβ4 and Tβ10, and the diacetylated on Lys16 and Lys 25 residues of Tβ4. These proteoforms have been previously characterized by our group in other human tissues and biological fluids by a top-down MS approach[49]. Other known proteoforms of thymosins[49,50] were unsuccessfully searched along the TIC profile.

Quantitative Evaluation of Tβ4 and Tβ10 in Tumor and Healthy Colon Mucosa

Concentration of Tβ4 and Tβ10 peptides and their derivatives was determined in deep and superficial tumor tissues and in healthy mucosa resected from 18 patients affected by CRC (Table III). Thus, 54 samples were analyzed in this study. In order to obtain the best comparison among the tissue samples, quantitative analysis did not consider the modified proteoforms of Tβ4 and Tβ10 sporadically detected in the <30 KDa protein fractions. Indeed, the percentage of Tβ4 modified proteoforms was 6% ± 5 (SD) of total Tβ4 in D tissue, 10% ± 9 in S tissue, and 12% ± 15 in H tissue. Tβ10 modified proteoforms were detected with the following percentages: 3% ± 3 in D, 5% ± 6 in S, and 4% ± 6 in H tissue. These percentages were not significantly different in the 18 patients.

Moreover, Tβ4 and Tβ10 were detected in both <30kDa and >30kDa protein fractions obtained by ultrafiltration of D, S and H samples. Indeed, in the fraction> 30kDa 25% ± 2 of Tβ4, and 25% ± 4 of Tβ10 were found. The results obtained by comparing the concentration of Tβ4 or Tβ10 in the fraction retained by the 30kDa cut-off membrane from D, S and H tissue samples appeared not significant (Table III). Conversely, statistically significant differences were obtained by considering the concentrations measured in <30kDa fractions, as well as the concentration given by the sum of <30kDa and >30kDa fractions (named in the following text "total Tβ4 and total Tβ10"). In particular, the concentration of both Tβ4 and Tβ10 was found significantly higher in deep tumor tissues with respect to the superficial ones. The result obtained by the statistical *t*-test (Table III) was confirmed by the ANOVA ($p < 0.05$). In the comparison of the two tumor tissues with respect to the healthy one, Tβ4 was found more concentrated in deep tumor tissues than in the healthy ones, but no differences were found be-

Table III. Concentration (mean and standard deviation) of Tβ4 and Tβ10 measured in superficial and deep tumor, and in healthy tissues resected from CRC patients, and results of the statistical comparison (*p* values). The analysis was performed by considering the concentration measured in each of the two protein fractions (<30 kDa and >30 kDa) both separately and their sum (total Tβ4 or Tβ10).

Peptide	Concentration (μM) mean ± SD			*t*-test *p* values		
	S	D	H	D *vs.* S	D *vs.* H	S *vs.* H
Tβ4 in < 30 kDa fractions	2.0 ± 1.3	3.4 ± 2.1	2.3 ± 1.4	0.001 ↑D	0.01 ↑D	ns
Tβ4 in > 30 kDa fractions	0.6 ± 0.6	1.0 ± 0.8	1.0 ± 0.7	ns	ns	ns
Total Tβ4	2.6 ± 1.7	4.3 ± 2.3	3.1 ± 1.5	0.0008 ↑D	0.03 ↑D	ns
Tβ10 in < 30 kDa fractions	0.5 ± 0.3	0.7 ± 0.4	0.6 ± 0.4	0.03 ↑D	0.04 ↑D	0.04 ↑H
Tβ10 in > 30 kDa fractions	0.2 ± 0.1	0.2 ± 0.2	0.2 ± 0.2	ns	ns	ns
Total Tβ10	0.6 ± 0.4	1.1 ± 0.7	0.8 ± 0.4	0.001 ↑D	0.03 ↑D	0.02 ↑H

tween superficial tumor and healthy tissues. The concentration of Tβ10 was found significantly lower in superficial tumor tissue with respect to both deep tumor and healthy tissues (Table III). The distribution of the total Tβ4 and Tβ10 concentrations measured in the three types of tissues is shown in Figure 1a and 1b, respectively. Tβ10 concentrations in deep and superficial tumor tissues maintained statistically significant differences (p = 0.0002) also by excluding the two higher values highlighted with arrows in Figure 1b.

Tβ4 and Tβ10 Concentrations, Dukes Stage and Budding Index

Total Tβ4 and total Tβ10 were also analyzed according to Dukes classification of the patients as A, B, and C stage. Figure 2a shows the scatter plot where Tβ4 concentrations measured in the deep tumor tissues are reported *vs.* those measured in the superficial tumor tissues. A similar plot for Tβ10 is shown in Figure 2b. Each point in the plots is labeled with a letter corresponding to the patient Dukes classification (A, B, and C). The cluster of Dukes'B patients showing the highest thymosin concentrations is evident in both plots.

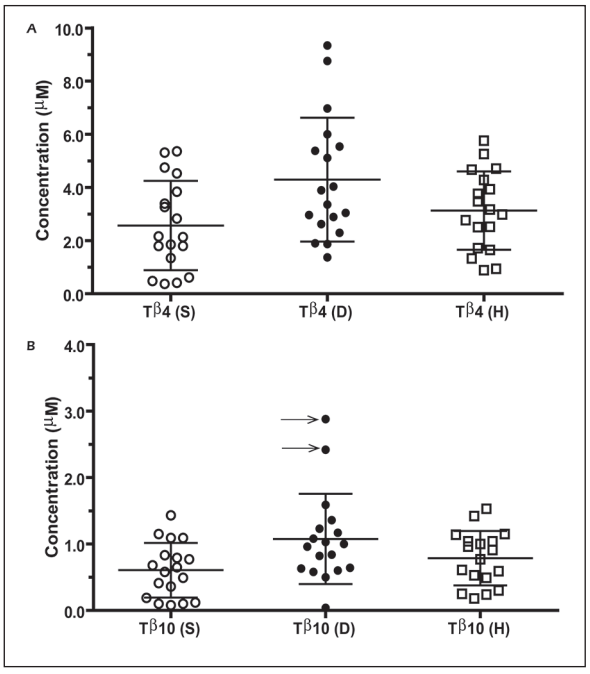

Figure 1. Distribution of the total concentration of Tβ4 **(A)** and Tβ10 **(B)** in the superficial (S), deep (D) tumor and healthy (H) tissues from 18 CRC patients.

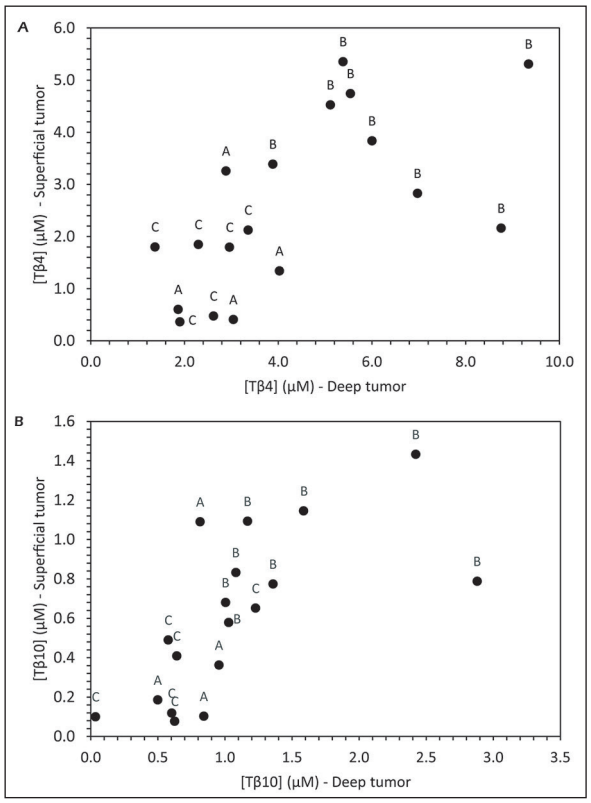

Figure 2. Scatter plot of Tβ4 **(A)** and Tβ10 **(B)** total concentrations measured in the deep tumor tissues are reported versus those measured in the superficial tumor tissues. Each point in the plots, is labeled with a letter corresponding to the patient Dukes'classification (A, B, and C).

Based on these preliminary considerations, we compared the concentrations of Tβ4 and Tβ10 measured in the total tumor samples (superficial and deep) from Dukes'B patients with those from Dukes'A and C patients (Table IV). Tumor tissues from Dukes'B stage patients showed a significant higher concentration of Tβ4 with respect to both Dukes'A and C patients. These results were confirmed also by the ANOVA analysis ($p < 0.01$ and < 0.001, respectively). Tβ10 was more abundant in tumor tissues from Dukes'B patients than in Dukes'A and C patients. Also, in this case the ANOVA analysis confirmed the results ($p < 0.05$ and $p < 0.0001$, respectively).

Analogously, we compared the concentration of Tβ4 and Tβ10 measured in the total tumor samples from each patient in relation to the budding index, ranged from 0 to 3. The highest abundance of both Tβ4 and Tβ10 was determined in the tumoral tissues of the three patients with discreet budding (index 2) and in two patients with index "1" (Figure 3a-b). It must

Table IV. Comparison between the concentrations (mean and standard deviation, and *p* values) of Tβ4 and Tβ10 measured in all the samples from CRC patients classified as A stage, B stage and C stage.

Peptide	Concentration (μM) mean ± SD			Mann-Whitney *p* value	
	A stage (n = 8 S, D)	B stage (n = 16 S, D)	C stage (n = 12 S, D)	B *vs.* A	B *vs.* C
Tβ4	2.2 ± 1.3	5.2 ± 1.9	1.9 ± 0.9	0.001 ↑B	< 0.0001 ↑B
Tβ10	0.6 ± 0.4	1.2 ± 0.6	0.5 ± 0.3	0.01 ↑B	0.0002 ↑B

be emphasized that these patients were all classified at Dukes stage B. The lowest thymosin's concentrations were found in the patients with budding index "0". The levels of Tβ4 in the subgroup with budding index "2" was significantly higher than in patients with index "0" and "1" ($p = 0.002$, and $p = 0.02$, respectively). Tβ10 was more expressed in patients with index "2" than in patients with index "0" and "3" ($p = 0.02$, and $p = 0.008$, respectively). The low number of patients did not allow to perform statistical analysis by considering the three different types of tissues, S, D, and H, in the subgroups of patients with different budding.

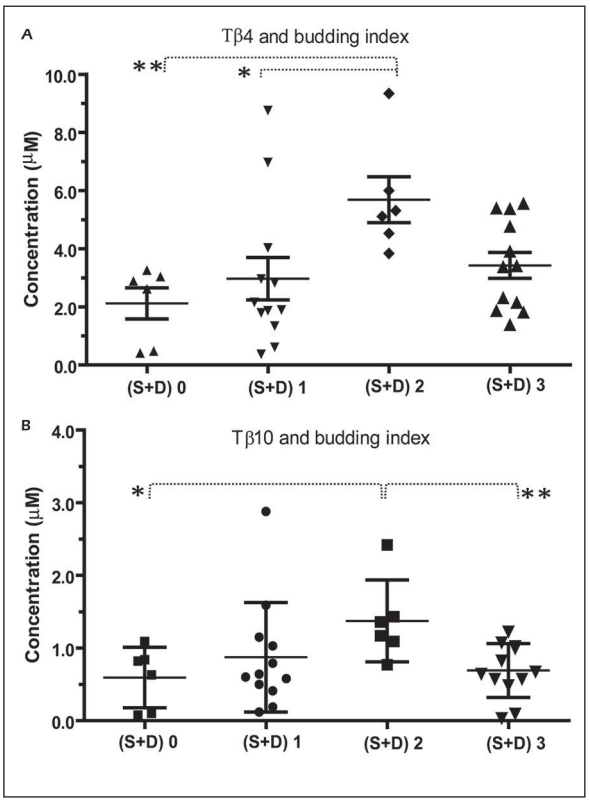

Figure 3. Distribution of the total concentration of Tβ4 **(A)** and Tβ10 **(B)** in relation to the budding index of the patients.

Discussion

Tβ4 and Tβ10 are peptides with a primary structure of 43 amino acid residues having high sequence homology, very conserved in mammalians[2]. Both peptides are Nα-acetylated after removal of the initial methionine and can undergo to many PTMs, such as proteolysis, iso-peptide crosslinking, Nε-acetylation of lysine residues, phosphorylation, and oxidation on methionine residue. The functional significance of the reactions listed above has not been fully understood[49,50]. In our samples, we identified the main forms of the two peptides, Tβ4 and Tβ10 Nα-acetylated, and several not abundant PTM forms, such as the Lys16,25-Nε-diacetylated Tβ4, the Met6-oxydized species of both Tβ4 and Tβ10, and two of the known proteolytic fragments of Tβ4 and Tβ10, namely Tβ4 1-41 and Tβ10 1-41. Huff et al[51] speculated that these truncated proteoforms of Tβ4 and Tβ10 might be generated *in vivo* by a carboxydipeptidase. Changes in the production of Tβ4 proteolytic fragments may be associated to immunological and tumor diseases[52]. Indeed, the levels of Tβ4 and Tβ10 proteolytic peptides were found increased in several malignant tumor histotypes[53]. Examples are pediatric brain tumors, such as medulloblastoma (high-grade tumor) and pilocytic astrocytoma (low-grade tumor)[54]. Nevertheless, the levels of Tβ4 1-41 and Tβ10 1-41, such as of the other modified forms detected in our samples, were negligible and did not result associated with CRC.

We determined the concentration of both thymosins in two areas of CRC tissues, the superficial and the deep section of the same tumor, and in the normal mucosa from 18 patients. The results highlighted marked differences in Tβ4 and Tβ10 concentration in relation to the area of the analyzed tumor: superficial, thus primitive, and deep, therefore, next to the front of tumor invasion. The two peptides were found significantly more abundant in the deep zones of the tumor, in

close proximity to the infiltrative tumor margins, with respect to the superficial tumor tissue and healthy mucosa. The higher concentration of Tβ4 in the deep tumor agreed with our previous data obtained on human colorectal cancer by immunohistochemical and molecular investigations[12]. In that study, we demonstrated that Tβ4 was markedly and preferentially expressed in tumor cells undergoing EMT in human colorectal cancer, particularly in close proximity to the deep infiltrative margins at the invasive front of the tumor. This evidence supported previous hypotheses for a role of T*β*4 in facilitating the progression of colon cancer[55]. Different mechanisms have been suggested to explain the action of Tβ4 in triggering EMT. For instance, the activation of laminin 5[56], metalloproteinases[27,57], or integrin-linked kinase (ILK) stimulate the ILK/*α*-threonine kinase/β-catenin signaling cascade[28-30]. This last event has been associated to a lower expression of E-cadherin, which is the principal cohesion factor of the epithelial cells. The overexpression and the nucleus-accumulation of β-catenin result in cell detachment, EMT and migration[30].

In the study of Nemolato et al[12], a progressive decrease of E-cadherin expression on the cell surface in Tβ4-reactive tumor cells undergoing EMT was analyzed. Furthermore, the loss of E-cadherin has been observed in isolated spindle tumor cells migrating toward lymphatic and/or blood vessels. Since E-cadherin principally mediates the loss of cell-cell adhesion causing tumor cell dispersion[58], it was hypothesized that T*β*4 may play a critical role in promoting EMT and leading to deregulation of cell-cell adhesion by downregulation of E-cadherin[12].

In our investigation we observed an association between the concentration of both Tβ4 and Tβ10 with the progression of the colorectal cancer classified by the Dukes stage, and the budding index, being this last parameter particularly connected with EMT in colorectal cancer. Indeed, EMT is evidenced by an alteration in tumor tissue architecture at the deep invasive tumor margins, which are referred as "budding margins," namely infiltrative margins with solid cell nests formed by 2-3 cancer cells that acquire motility and infiltrate the peritumoral connective tissue[59].

Interestingly, our investigation found the major concentration of Tβ4 in the tumor tissue samples of the patients at Dukes stage B, and thus, characterized by a cancer diffusion *via* direct continuity to the extra-rectal tissue. By considering the budding index, the highest concentration of Tβ4 was determined in the three patients at B stage with budding index "2", and in two patients at Dukes stage B with budding index "1". These findings, even if limited by the low number of samples, suggested that the difference in Tβ4 concentration could discriminate patients at Dukes stage B from the others. Moreover, the association with the budding index, particularly in patients at Dukes stage B, supports the hypothesis that Tβ4 may participate in the promotion of EMT in colorectal cancer. The present study showed that also Tβ10 could be involved in the progression of CRC and its propensity to metastasize. Our results showed that Tβ10 concentrations varied similarly to Tβ4, being higher in the deep tumor tissue zones than in the superficial areas. Furthermore, the results revealed that Tβ4 and Tβ10 could represent good potential biomarker candidates to discriminate patients at stage B and with budding index "2".

This evidence appeared to be of interest, taking into consideration the intra-tumor heterogeneity, one of the factors mainly contributing to the development of precision medicine in colorectal cancer[60]. A more precise stratification of patients has shown higher response rate (ORR), longer progression-free survival (PFS) and median overall survival (OS), and less hematological and extra-hematological toxicities[61,62,63].

In particular, the prognostic-predictive serum and tissue markers have changed the picture in CRC by chiefly leading the oncologist therapeutic approach together with improving the understanding of colorectal cancer biology[64,65,66,67]. From this point of view, the discovery of clinically relevant protein biomarkers correlated to intra-tumor heterogeneity were suggested to be promising for its clinical applications in the diagnosis, prognosis, and treatment of CRC[68]. Indeed, the different distribution of Tβ4, and Tβ10, in the superficial and deep zones of the tumor, was in accordance with the intra-tumoral heterogeneity typical of the colorectal cancer observed in several previous studies at transcriptomic and proteomic level[68,69].

Conclusions

Since beta-thymosin family has been demonstrated to play a main physiological role in the regulation of actin polymerization, angiogenesis, cell survival, and cell migration, we analyzed Tβ4 and Tβ10, the two most abundant members of this family, in CRC[70].

The present investigation highlighted that both thymosins, Tβ4 and Tβ10, exhibited intra-tumor quantitative differences, being upregulated in the deep part of the CRC. The observed association between the concentration of both Tβ4 and Tβ10 with the Dukes stage and the budding grade, suggests that the two thymosins are involved in colorectal cancer progression, and in the promotion of cancer invasion. Therefore, Tβ4 and Tβ10 are good candidates to be diagnostic-prognostic biomarkers and therapeutic targets.

Conflict of Interest

The Authors declare that they have no conflict of interests.

Funding

The study was supported by Regione Sardegna funds: Progetti Ricerca di base orientata -L.R. 7/2007- year 2012, F71J12000850002, Coordinator: Tiziana Cabras

References

1) Goldstein AL, Slater FD, White A. Preparation, assay, and partial purification of a thymic lymphocytopoietic factor (thymosin). Proc Natl Acad Sci USA 1966; 21: 1010-1017.
2) Hannappel E. beta-Thymosins. Ann NY Acad Sci 2007; 1112: 21-37.
3) Huff T, Müller CSG, Otto AM, Netzker R, Hannappel E. β-thymosins, small acidic peptides with multiple functions. Int J Biochem Cell Biol 2001; 33: 205-220.
4) Faa G, Fanos V. Current Clinical Pathology. Springer Science New York, 2014, 81-92.
5) Mannherz HG, Hannappel E. The beta-thymosins: intracellular and extracellular activities of a versatile actin binding protein family. Cell Motility and the Cytoskeleton 2009; 66: 839-851.
6) Kuzan A. Thymosin β as an Actin-binding Protein with a Variety of Functions. Adv Clin Exp Med 2016; 25: 1331-1336.
7) Sribenja S, Wongkham S, Wongkham C, Yao Q, Chen C. Roles and mechanisms of β-thymosins in cell migration and cancer metastasis: an update. Cancer Invest 2013; 31: 103-110.
8) Faa G, Nemolato S, Cabras T, Fanni D, Gerosa C, Fanari M, Locci A, Fanos V, Messana I, Castagnola M. Thymosin β4 expression reveals intriguing similarities between fetal and cancer cells. Ann N Y Acad Sci 2012; 1269: 53-60.
9) Can B, Karagoz F, Yildiz L, Yildirim A, Kefeli M, Gonullu G, Kandemir B. Thymosin β4 is a novel potential prognostic marker in gastrointestinal stromal tumors. APMIS 2012; 120: 689-698.
10) Theunissen W, Fanni D, Nemolato S, Di Felice E, Cabras T, Gerosa C, Van Eyken P, Messana I, Castagnola M, Faa G. Thymosin beta 4 and thymosin beta 10 expression in hepatocellular carcinoma. Eur J Histochem 2014; 58: 2242.
11) Ricci-Vitiani L, Mollinari C, di Martino S, Biffoni M, Pilozzi E, Pagliuca A, de Stefano MC, Circo R, Merlo D, De Maria R, Garaci E. Thymosin beta4 targeting impairs tumorigenic activity of colon cancer stem cells. FASEB J 2010; 24: 4291-4301.
12) Nemolato S, Restivo A, Cabras T, Coni P, Zorcolo L, Orrù G, Fanari M, Cau F, Gerosa C, Fanni D, Messana I, Castagnola M, Casula G, Faa G. Thymosin β4 in colorectal cancer is localized predominantly at the invasion front in tumor cells undergoing epithelial mesenchymal transition. Cancer Biol Ther 2012; 13: 191-197.
13) Kang YJ, Jo JO, Ock MS, Chang HK, Lee SH, Ahn BK, Baek KW, Choi YH, Kim WJ, Leem SH, Cha HJ. Thymosin β4 was upregulated in recurred colorectal cancers. J Clin Pathol 2014; 67: 188-190.
14) Gemoll T, Strohkamp S, Schillo K, Thorns C, Habermann JK. MALDI-imaging reveals thymosin beta-4 as an independent prognostic marker for colorectal cancer. Oncotarget 2015; 6: 43869-43880.
15) Yiu AJ, Yiu CY. Biomarkers in Colorectal Cancer. Anticancer Res 2016; 36: 1093-1102.
16) Farooqi AA, de la Roche M, Djamgoz MBA, Siddik ZH. Overview of the oncogenic signaling pathways in colorectal cancer: Mechanistic insights. Semin Cancer Biol 2019; 58: 65-79.
17) Cha HJ, Jeong MJ, Kleinman HK. Role of Thymosin β4 in tumor metastasis and angiogenesis. J Natl Cancer Inst 2003; 95: 1674-1680.
18) Yoon SY, Lee HR, Park Y, Kim JH, Kim SY, Yoon SR, Lee WJ, Cho BJ, Min H, Bang JW, Park H, Bang SI, Cho D. Thymosin β4 expression correlates with lymph node metastasis through hypoxia inducible factor-α induction in breast cancer. Oncol Rep 2011; 25: 23-31.
19) Lee JW, Ryu YK, Ji YH, Kang JH, Moon EY. Hypoxia/reoxygenation-experienced cancer cell migration and metastasis are regulated by Rap1- and Rac1-GTPase activation via the expression of thymosin beta-4. Oncotarget 2015; 6: 9820-9833.
20) Kim NS, Kang YJ, Jo JO, Kim HY, Oh YR, Kim YO, Jung MH, Ock MS, Cha HJ. Elevated expression of thymosin β4, vascular endothelial growth factor (VEGF), and hypoxia inducible factor (HIF)-1α in early-stage cervical cancers. Pathol Oncol Res 2011; 17: 493-502.
21) Wei C, Kumar S, Kim IK, Gupta S. Thymosin beta 4 protects cardiomyocytes from oxidative stress by targeting anti-oxidative enzymes and anti-apoptotic genes. PLoS One 2012; 7: e42586.
22) Moon EY, Song JH, Yang KH. Actin-sequestering protein, thymosin-beta-4 (TB4), inhibits

caspase-3 activation in paclitaxel-induced tumor cell death. Oncol Res 2007; 16: 507-516.

23) Kumar S, Gupta S. Thymosin beta 4 prevents oxidative stress by targeting antioxidant and anti-apoptotic genes in cardiac fibroblasts. PLoS One 2011; 6: e26912.

24) Goldstein AL. Thymosin beta4: a new molecular target for antitumor strategies. J Natl Cancer Inst 2003; 95: 1646-1647.

25) Xiao Y, Chen Y, Wen J, Yan W, Zhou K, Cai W. Thymosin β4: a potential molecular target for tumor therapy. Crit Rev Eukaryot Gene Expr 2012; 22: 109-116.

26) Hong KO, Lee JI, Hong SP, Hong SD. Thymosin β4 induces proliferation, invasion, and epithelial-to-mesenchymal transition of oral squamous cell carcinoma. Amino Acids 2016; 48: 117-127.

27) Cierniewski CS, Papiewska-Pajak I, Malinowski M, Sacewicz-Hofman I, Wiktorska M, Kryczka J, Wysocki T, Niewiarowska J, Bednarek R. Thymosin beta4 regulates migration of colon cancer cells by a pathway involving interaction with Ku80. Ann N Y Acad Sci 2010; 1194: 60-71.

28) Tang MC, Chan LC, Yeh YC, Chen CY, Chou TY, Wang WS, Su Y. Thymosin beta 4 induces colon cancer cell migration and clinical metastasis via enhancing ILK/IQGAP1/Rac1 signal transduction pathway. Cancer Lett 2011; 308: 162-171.

29) Huang HC, Hu CH, Tang MC, Wang WS, Chen PM, Su Y. Thymosin beta4 triggers an epithelial-mesenchymal transition in colorectal carcinoma by upregulating integrin-linked kinase. Oncogene 2007; 26: 2781-2790.

30) Piao Z, Hong CS, Jung MR, Choi C, Park YK. Thymosin β4 induces invasion and migration of human colorectal cancer cells through the ILK/AKT/β-catenin signaling pathway. Biochem Biophys Res Commun 2014; 452: 858-864.

31) Wang WS, Chen PM, Hsiao HL, Wang HS, Liang WY, Su Y. Overexpression of the thymosin beta-4 gene is associated with increased invasion of SW480 colon carcinoma cells and the distant metastasis of human colorectal carcinoma. Oncogene 2004; 23: 6666-6671.

32) Sribenia S, Li M, Wongkham S, Wongkham C, Yao Q, Chen C. Advances in thymosin beta10 research: differential expression, molecular mechanisms, and clinical implications in cancer and other conditions. Cancer Investig 2009; 27: 1016-1022.

33) Lee SH, Son MJ, Oh SH, Rho SB, Park K, Kim YJ, Park MS, Lee JH. Thymosin beta 10 inhibits angiogenesis and tumor growth by interfering with Ras function. Cancer Res 2005; 65: 137-148.

34) Mu H, Ohashi R, Yang H, Wang X, Li M, Lin P, Yao Q, Chen C. Thymosin beta 10 inhibits cell migration and capillary-like tube formation of human coronary artery endothelial cells. Cell Motil Cytoskeleton 2006; 63: 222-230.

35) Hall AK. Thymosin beta-10 accelerates apoptosis. Cell Mol Biol Res 1995; 41: 167-180.

36) Kim YC, Kim BG, Lee JH. Thymosin β10 expression driven by the human TERT promoter induces ovarian cancer-specific apoptosis through ROS production. PLoS One 2012; 7: e35399.

37) Sribenja S, Sawanyawisuth K, Kraiklang R, Wongkham C, Vaeteewoottacharn K, Obchoei S, Yao Q, Wongkham S, Chen C. Suppression of thymosin β10 increases cell migration and metastasis of cholangiocarcinoma. BMC Cancer 2013; 13: 430.

38) Zhang X, Ren D, Guo L, Wang L, Wu S, Lin C, Ye L, Zhu J, Li J, Song L, Lin H, He Z. Thymosin beta 10 is a key regulator of tumorigenesis and metastasis and a novel serum marker in breast cancer. Breast Cancer Res 2017; 19: 15.

39) Bouchal P, Dvořáková M, Roumeliotis T, Bortlíček Z, Ihnatová I, Procházková I, Ho JT, Maryáš J, Imrichová H, Budinská E, Vyzula R, Garbis SD, Vojtěšek B, Nenutil R. Combined Proteomics and Transcriptomics Identifies Carboxypeptidase B1 and Nuclear Factor κB (NF-κB) Associated Proteins as Putative Biomarkers of Metastasis in Low Grade Breast Cancer. Mol Cell Proteomics 2015; 14: 1814-1830.

40) Li M, Zhang Y, Zhai Q, Feurino LW, Fisher WE, Chen C, Yao Q. Thymosin beta-10 is aberrantly expressed in pancreatic cancer and induces JNK activation. Cancer Invest 2009; 27: 251-256.

41) Gu Y, Wang C, Wang Y, Qiu X, Wang E. Expression of thymosin beta10 and its role in non-small cell lung cancer. Hum Pathol 2009; 40: 117-124.

42) Santelli G, Califano D, Chiappetta G, Vento MT, Bartoli PC, Zullo F, Trapasso F, Viglietto G, Fusco A. Thymosin beta-10 gene overexpression is a general event in human carcinogenesis. Am J Pathol 1999; 155: 799-804.

43) Koelzer VH, Zlobec I, Lugli A. Tumor budding in colorectal cancer—ready for diagnostic practice? Human Pathology 2016; 47; 4-19.

44) Zhang Z, Marshall AG. A universal algorithm for fast and automated charge state deconvolution of electrospray mass-to-charge ratio spectra. J Am Soc Mass Spectrom 1998; 9: 225-233.

45) Ong SE, Mann M. Mass spectrometry-based proteomics turns quantitative. Nat Chem Biol 2005; 1: 252-262.

46) Messana I, Inzitari R, Fanali C, Cabras T, Castagnola M. Facts and artifacts in proteomics of body fluids. What proteomics of saliva is telling us? J Sep Sci 2008; 31: 1948-1963.

47) Perez-Riverol Y, Csordas A, Bai J, Bernal-Llinares M, Hewapathirana S, Kundu DJ, Inuganti A, Griss J, Mayer G, Eisenacher M, Pérez E, Uszkoreit J, Pfeuffer J, Sachsenberg T, Yilmaz S, Tiwary S, Cox J, Audain E, Walzer M, Jarnuczak AF, Ternent T, Brazma A, Vizcaíno JA. The PRIDE database and related tools and resources in 2019: improving support for quantification data. Nucleic Acids Res 2019; 47: D442-D450.

48) Deutsch EW, Bandeira N, Sharma V, Perez-Riverol Y, Carver JJ, Kundu DJ, García-Seisde-

dos D, Jarnuczak AF, Hewapathirana S, Pullman BS, Wertz J, Sun Z, Kawano S, Okuda S, Watanabe Y, Hermjakob H, MacLean B, MacCoss MJ, Zhu Y, Ishihama Y, Vizcaíno JA. The ProteomeXchange consortium in 2020: enabling 'big data' approaches in proteomics, Nucleic Acids Res 2020; 48: D1145-D1152.

49) Cabras T, Iavarone F, Martelli C, Delfino D, Rossetti DV, Inserra I, Manconi B, Desiderio C, Messana I, Hannappel E, Faa G, Castagnola M. High-resolution mass spectrometry for thymosins detection and characterization. Expert Opin Biol Ther 2015; 15: S191-201.

50) Hannappel E. Thymosin beta4 and its posttranslational modifications. Ann NY Acad Sci 2010; 1194: 27-35.

51) Huff T, Müller CSG, Hannappel E. C-terminal truncation of thymosin β10 by an intracellular protease and its influence on the interaction with G-actin studied by ultrafiltration. Febs Letters 1997; 414: 39-44.

52) Plavina T, Hincapie M, Wakshull E, Subramanyam M, Hancock WS. Increased plasma concentrations of cytoskeletal and Ca2+-binding proteins and their peptides in psoriasis patients. Clin Chem 2008; 54: 1805-1814.

53) Hardesty WM, Kelley MC, Mi D, Low R, Caprioli RM. Protein signatures for survival and recurrence in metastatic melanoma. J Proteomics 2011; 74: 1002-1014.

54) Martelli C, Iavarone F, D'Angelo L, Arba M, Vincenzoni F, Inserra I, Delfino D, Rossetti DV, Caretto M, Massimi L, Tamburrini G, Di Rocco C, Caldarelli M, Messana I, Castagnola M, Sanna MT, Desiderio C. Integrated proteomic platforms for the comparative characterization of medulloblastoma and pilocytic astrocytoma pediatric brain tumors: a preliminary study. Mol Biosyst 2015; 11: 1668-1683.

55) Larsson LI, Holck S. Localization of thymosin beta-4 in tumors. Ann N Y Acad Sci 2007; 1112: 317-325.

56) Sosne G, Xu L, Prach L, Mrock LK, Kleinman HK, Letterio JJ, Hazlett LD, Kurpakus-Wheater M. Thymosin beta 4 stimulates laminin-5 production independent of TGF-beta. Exp Cell Res 2004; 293: 175-183.

57) Qiu P, Kurpakus-Wheater M, Sosne G. Matrix metalloproteinase activity is necessary for thymosin beta 4 promotion of epithelial cell migration. J Cell Physiol 2007; 212: 165-173.

58) Wijnhoven BPL, Dinjens WN, Pignatelli M. E-cadherincatenin cell-cell adhesion complex and human cancer. Br J Surg 2000; 87: 992-1005.

59) Ogawa T, Yoshida T, Tsuruta T, Tokuyama W, Adachi S, Kikuchi M, Mikami T, Saigenji K, Okayasu I. Tumor budding is predictive of lymphatic involvement and lymph node metastases in submucosal invasive colorectal adenocarcinomas and in non polypoid compared with polypoid growth. Scand J Gastroenterol 2009; 4: 605-614.

60) Seoane J, De Mattos-Arruda L. The challenge of intratumour heterogeneity in precision medicine. J Intern Med 2014; 276: 41-51.

61) Berretta M, Cappellani A, Fiorica F, Nasti G, Frustaci S, Fisichella R, Bearz A, Talamini R, Lleshi A, Tambaro R, Cocciolo A, Ristagno M, Bolognese A, Basile F, Meneguzzo N, Berretta S, Tirelli U. FOLFOX4 in the treatment of metastatic colorectal cancer in elderly patients: a prospective study. Arch Gerontol Geriatr 2011; 52: 89-93.

62) Fiorica F, Cartei F, Carau B, Berretta S, Spartà D, Tirelli U, Santangelo A, Maugeri D, Luca S, Leotta C, Sorace R, Berretta M. Adjuvant radiotherapy on older and oldest elderly rectal cancer patients. Arch Gerontol Geriatr 2009; 49: 54-59.

63) Goodarzi E, Beiranvand R, Naemi H, Momenabadi V, Khazaei Z. Worldwide incidence and mortality of colorectal cancer and human development index (HDI): an ecological study. WCRJ 2019; 6: e1433).

64) Berretta M, Alessandrini L, De Divitiis C, Nasti G, Lleshi A, Di Francia R, Facchini G, Cavaliere C, Buonerba C, Canzonieri V. Serum and tissue markers in colorectal cancer: State of art. Crit Rev Oncol Hematol 2017; 111: 103-116.

65) Zhang DL, Yang N. MiR-3174 functions as an oncogene in rectal cancer by targeting PCBD2. Eur Rev Med Pharmacol Sci 2019; 23: 2417-2426.

66) Nappi A, Nasti G, Romano C, Berretta M, Ottaiano A. Metastatic Colorectal Cancer: Prognostic and Predictive Factors. Curr Med Chem 2020; 27: 2779-2791.

67) Torshizi EA, Seyedna SY, Nazemalhosseini ME, Majd A, Asadzadeh AH. TGF-β/Smad signaling pathway as a candidate for EMAST phenotype in colorectal cancer patients. WCRJ 2020; 7: e1470.

68) Lim LC, Lim YM. Proteome Heterogeneity in Colorectal Cancer. Proteomics 2018; 18: 1-9.

69) Árnadóttir SS, Mattesen TB, Vang S, Madsen MR, Madsen AH, Birkbak NJ, Bramsen JB, Andersen CL. Transcriptomic and proteomic intra-tumor heterogeneity of colorectal cancer varies depending on tumor location within the colorectum. PLoS One 2020; 15: e0241148.

70) Faa G, Piras M, Mancuso L, Coni P, Pichiri G, Orrù G, Fanni D, Gerosa C, Cao G, Taibi R, Pavone P, Castagnola M. Thymosin beta-4 prenatal administration improves fetal development and halts side effects due to preterm delivery. Eur Rev Med Pharmacol Sci 2021; 25: 431-437.